Comm. Korean Math. Soc. **16** (2001), No. 3, pp. 445–458

PROBLEMS IN INVERSE SCATTERING-ILLPOSEDNESS, RESOLUTION, LOCAL MINIMA, AND UNIQUENESSE

JUNG-WOONG RA

ABSTRACT. The shape and the distribution of material construction of the scatterer may be obtained from its scattered fields by the iterative inversion in the spectral domain. The illposedness, the resolution, and the uniqueness of the inversion are the key problems in the inversion and inter-related. The illposedness is shown to be caused by the evanescent modes which carries and amplifies exponentially the measurement errors in the back-propagation of the measured scattered fields. By filtering out all the evanesce nt modes in the cost functional defined as the squared differrence between the mesured and the calculated spatial spectrum of the scattered fields from the iteratively chosen medium parameters of the scatterer, one may regularize the illposedness of the inversion in the expense of the resolution. There exist many local minima of the cost functional for the inversion of the large and the high-contrast scatterer and the hybrid algorithm combining the genetic algorithm and the Levenberg-Marquardt algorithm is shown to find efficiently its global minimum. The resolution of reconstruction obtained by keeping all the propating modes and filtering out the evanescent modes for the regularization becomes 0.5 wavelength. The super resolution may be obtained by keeping the evanescent modes wnen the measurement error and distance, respectively, are small and near.

1. Introduction

The shape and material parameters such as the complex permittivities and permeabilities of an object may be reconstructed from the fields scattered by the object. For a small and low contrasted object, the Born

Received January 11, 2001.
2000 Mathematics Subject Classification: 65O99.
Key words and phrases: inverse, scattering, illposedness, resolution, local minima, uniquenesse.

approximation [1] linearizes the relation between the permittivity distribution and the scattered field by approximating the total field inside the penetrable scattering object by its incident field.

For high contrasted object where permitivities of the object are much different from the host medium, the moment method inversion [2] may be used to discretize the object into small cells much smaller than the wavelength, such that the fields in each cell may be assumed constant, and then to obtain the polarization current in each cell from the scattered fields. The total field inside the object is obtained from the polarization currents, and the distribution of the permittivity is then obtained by taking the ratio of the polarization current and the total field in each cell. This moment method inversion, however, is shown to suffer from the "illposedness"[3] in a sense that a small error in the scattered fields causes a large error in the polarization currents. The cause of this illposedness may be identified as the exponentially decaying behavior of the evanescent modes, which makes the small error in the evanescent modes of the scattered fields grow exponentially in the back propagating process of the inversion [4].

By selecting only the propagating modes excluding the evanescent modes in the spectrum of the measured scattered fields, the illposedness is regularized without the extra regularization terms of Tikhonov [3] nor the use of the pseudo-inversion, which needs much more measured data points than needed [5]. For a large scatterer producing fewer propagating modes P than the number of unknowns N, the total number of cells discretizing the object, the moment method inversion does not give the right reconstruction of the object even with many multiple incident waves, since the polarization currents in each cell vary with different incident waves. Iterative inversion is more effective for this type of reconstruction. One may define a cost functional as the summation of the squared magnitude of the difference between the measured and the calculated scattered fields from the iteratively chosen dielectric profiles. One then minimizes this cost functionals by utilizing the optimizing algorithms such as Levenberg-Marquardt algorithm [6], simulated annealing algorithm [7], and genetic algorithm [8].

The Levenberg-Marquardt (**LM**) algorithm alone is good enough to reconstruct the low contrasted and small object satisfying the criterion of Born approximation. One needs the stochastic algorithms such as the simulated annealing (**SA**) algorithm or the genetic (**GE**) algorithm to find the global minimum in reconstructing a large and high contrasted

object, since there exists many local minima in its cost functional [9]. A hybrid algorithm combining **LM** and **SA** [9] or **GE** [10] is effective in finding the global minimum of the cost functional. Regularization is needed for the iterative inversion and the spectral domain filtering of evanescent modes is effective as in the moment method inversion [9, 10].

Super resolution seems to be obtainable in the reconstruction of the object since the discretization of the object seems to be arbitrary. However, the super resolution requires proper measurement of the scattered fields including evanescent fields which may cause the illposedness in the process of inversion. The scattered fields may be represented as a superposition of plane waves, i.e. the Fourier transformation of the field, say in y-direction, and transformed back, say in z-direction, to the plane of object. The resolution of the reconstruction of the object in the y-direction, say Δy, may then be obtained from the sampling theorem, $\Delta y \cdot \Delta k = 2\pi$, where Δk is the bandwidth of the spatial frequency of the fields in the object plane in the y-direction, which is the same with that of the measured scattered fields. Measurement of all the propagating modes gives $\Delta k \leq 2k_0$, where k_0 is the wave number of the background medium, and the maximum resolution becomes $\Delta y \geq 1/2\lambda$, where λ is the wavelength. For the super resolution such as $\Delta y \sim 0.1\lambda, \Delta k >> k_0$ is needed and it means the measurement of the evanescent mode fields in addition to the propagating modes.

Non-uniqueness of the inverse solution is often mentioned, by arguing the existence of non-radiating sources. In addition, the existence of the inverse solution is questionable due to the illposedness of the inverse problems. One may filter out the contribution of evanescent modes in the scattered fields at the expense of the resolution of the reconstruction, which regularizes inversion process. One may show that the unique reconstruction of the profile parameters of the penetrable object up to that resolution from the scattered field is possible by the iterative inversion.

2. Illposedness of inversion

When a time harmonic plane wave having a z-polarized electric field is incident upon a two-dimensional dielectric cylinder of arbitrary cross section along the z axis, the total field satisfies the inhomogeneous Helmholtz equation with the source term producing the incident plane wave. If the cross section of the object is given by its distribution of relative permittivities $\epsilon(\boldsymbol{\rho})$, where $\boldsymbol{\rho}$ is the two-dimensional cylindrical coordinate vectors, the total fields polarized in the z direction may be

represented by the sum of the incident wave and the scattered wave, u^s [11],

$$u^S(\boldsymbol{\rho}) = k_0^2 \iint_{S_0} d\boldsymbol{\rho}'[\epsilon(\boldsymbol{\rho}') - 1]u(\boldsymbol{\rho})G(\boldsymbol{\rho}, \boldsymbol{\rho}'), \tag{1}$$

where k_0 is the wave number in the background medium, u is the total field inside the dielectric cylinder S_0, $\boldsymbol{\rho}$ and $\boldsymbol{\rho}'$ are the cylindrical or rectangular coordinate vectors and G is the two-dimensional Green's function. The radiation condition for u^S is satisfied by $G(\boldsymbol{\rho}, \boldsymbol{\rho}')$, and G may be represented either in the configuration or the spectral domain as

$$G(\boldsymbol{\rho}, \boldsymbol{\rho}') = -(j/4)H_0^{(2)}(k_0|\boldsymbol{\rho} - \boldsymbol{\rho}'|), \tag{2a}$$

$$= -(j/4) \sum_{m=-\infty}^{\infty} J_m(k_0\rho')H_m^{(2)}(k_0\rho)e^{jm(\phi-\phi')}, \ \rho > \rho', \tag{2b}$$

$$= \frac{1}{2\pi} \int_{-\infty}^{\infty} d\beta e^{-j\beta(y-y')} \frac{e^{-j\sqrt{k_0^2-\beta^2}|x-x'|}}{2j\sqrt{k_0^2-\beta^2}}, \tag{2c}$$

where J_m and $H_m^{(2)}$ are the mth order Bessel function and Hankel function of the second kind, respectively, for the time dependence $e^{j\omega t}$.

One may calculate the scattered fields numerically by using the moment method [12] by dividing the cross section S_0 into small cells smaller than $0.2\lambda/\sqrt{\epsilon}$, where λ is the free space wavelength. The size of the cell is small enough that the polarization current inside each cell is taken as a constant. Substituting (2) into (1), one obtains the integral in (1) for the scattered field by the summation over the total number of cells N, as

$$u^S(\boldsymbol{\rho}) = \sum_{n=1}^{N} [\epsilon_n(\boldsymbol{\rho}_n) - 1]u_n(\boldsymbol{\rho}_n)I_n(\boldsymbol{\rho}, \boldsymbol{\rho}_n), \tag{3}$$

where ϵ_n and u_n are the relative permittivity and the total field at $\boldsymbol{\rho} = \boldsymbol{\rho}_n$, respectively,

$$\begin{aligned} I_n(\boldsymbol{\rho}, \boldsymbol{\rho}_n) = & -(j\pi/2)k_0 a J_1(k_0 a) \\ & \sum_{m=-\infty}^{\infty} e^{jm\phi} H_m^{(2)}(k_0\rho)J_m(k_0\rho_n)e^{-jm\phi_n}, \quad \rho > \rho' \end{aligned} \tag{4}$$

and

$$I_n(\boldsymbol{\rho},\boldsymbol{\rho}_n) = \frac{1}{2\pi}\int_{-\infty}^{\infty} d\beta e^{-j\beta(y-y_n)}\frac{e^{-j\sqrt{k_0^2-\beta^2}|x-x_n|}}{2j\sqrt{k_0^2-\beta^2}} \times (2k_0 d)\frac{\sin\beta d}{\beta d}\frac{\sin(\sqrt{k_0^2-\beta^2}d)}{\sqrt{k_0^2-\beta^2}d} \tag{5}$$

from the spectral domain Green's function in (2b) and (2c), respectively, where Graf's integral theorem [13] of Bessel functions is used in the process of the integral evaluation of (1) and (2b). [14]

To find $\epsilon(\boldsymbol{\rho})$ from the integral in (1) is a nonlinear problem. This inversion problem is shifted into finding the polarization current, $(\epsilon_n - 1)u_n$, in (3) from the measured scattered field $u^S(\boldsymbol{\rho})$ for the same number of measurement points with the total number of cells, $\boldsymbol{\rho} = \boldsymbol{\rho}_l$, $l = 1, 2, \cdots, N$. This problem becomes linear and its solution is unique if I_n is well defined, where I_n depends upon the geometrical configuration of the discretized cells and measurement points, $|\boldsymbol{\rho}_l - \boldsymbol{\rho}_n| = \rho_{ln}$. Since the cells are discretized much smaller than the wavelength, ρ_{ln} does not change much for the neighboring $(n+1)$th cell, and the values of the neighboring column of the matrix $I_n(\rho_{ln})$ are not much different from $I_n(\rho_{ln+1})$. This makes the inversion of the matrix I_n from (3) in the configuration domain unstable. If there exists a very small error in the measurement of the scattered field u^S, it causes uncontrollable error in the calculation of $(\epsilon_n - 1)u_n$. This is generally known as the illposedness of Hadamard, and the quadratic constraint [15] in the sense of Tikhonov has been used to regularize the illposedness. Thus, the configuration domain inversion of the polarization current needs an additional regularization term [16] in the inversion of the matrix I_n to compromise the errors in the resultant polarization currents and the stabilization of the inversion process.

3. Iterative inversion in the spectral domain

One may utilize the additional data points generated by using multiple incidences and frequencies of the source via the iterative inversion. The cost functional may be defined as the summation of the squared magnitude of the difference fields between the measured fields and the fields calculated from the assumed set of dielectric profiles for the iterations. One then minimizes this cost functional iteratively by updating the distribution of the complex permittivity profile until the original

distribution of the complex permittivity is found.

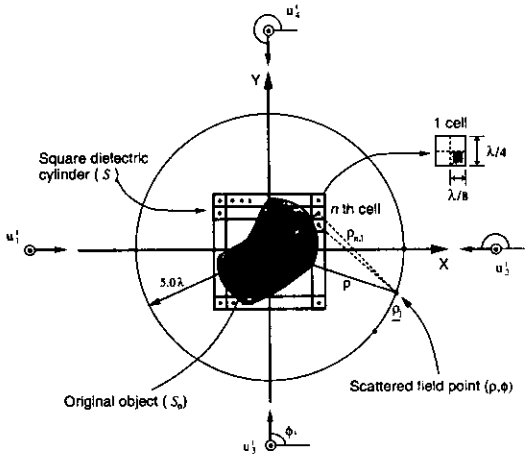

FIGURE 1. Plane wave incidence on an arbitrary object which is estimated by the square dielectric cylinder in the inversion.

The cost functional f may be defined as

$$f = \frac{1}{2}\sum_{i=1}^{I}\sum_{j=1}^{J}\int_0^{2\pi} d\phi \left| u_M^S(\rho,\phi;\omega_i,\phi_j) - u_C^S(\rho,\phi;\omega_i,\phi_j;\epsilon_n)\right|^2, \tag{6}$$

where u_M^S and u_C^S are, respectively, the measured and the calculated scattered fields from the distribution ϵ_n, I and J are the total number of angular frequencies(ω_i), and their incident angles(ϕ_j), respectively, and the squared difference fields are integrated over angular angle ϕ in the measurement cylindrical surface of $\rho =$ constant as shown in Figure 1. The measurement error and noise may be included in u_M^S. One may convert this functional in the configuration domain into that in the spectral domain by using the Green's function given in (2b) for the cylindrical measurement.

Substituting (3) and (4) into (6), the integration over ϕ makes the double summation over m in (4) into the single summation which may be taken outside of the squared magnitude of F_{mij} as

$$f = \frac{1}{2}\sum_{i=1}^{I}\sum_{j=1}^{J}\sum_{m=-\infty}^{\infty} |F_{mij}|^2, \tag{7}$$

where

$$F_{mij} = H_m^{(2)}(k_0\rho)\Big\{\frac{a_m(\rho;\omega_i,\phi_j)}{H_m^{(2)}(k_0\rho)} - \frac{j\pi k_0 a}{2}J_1(k_0 a) \cdot \sum_{n=1}^{N}(\epsilon_n - 1)u_n(\omega_i;\phi_j)J_m(k_0\rho_n)e^{-jm\phi_n}\Big\}, \tag{8}$$

the second term in (8) is obtained from (3) and (4) and

$$a_m(f;\omega_i,\phi_j) = \frac{1}{2\pi}\int_0^{2\pi} d\phi u_M^S(\rho,\phi;\omega_i,\phi_j)e^{-jm\phi}. \tag{9}$$

The cause of the illposedness may be explained from the behavior of the product $H_m^{(2)}(k_0\rho)J_m(k_0\rho_n)$ in (4) and (7). When a white Gaussian noise distribution is assumed in the scattered field, the noise power distributed over the modes is uniform. The modal amplitudes of the noiseless scattered field decrease fast for higher modes of $|m| > M$. For the inversion, these scattered fields with noise are transformed into the scattered fields inside the scatterer in which the back propagation via the $H_m^{(2)}(k_0\rho)$ is needed, where $H_m^{(2)}(k_0\rho)$ diverges fast in the near field range, $k_0\rho << m$, $m > 0$, as

$$H_m^{(2)}(k_0\rho_n) \sim \frac{1}{\sqrt{2\pi m}}\left(\frac{ek_0\rho_n}{2m}\right)^m, \; m >> k_0\rho. \tag{10}$$

This diverging process amplifies the noise existing in the scattered field in the process of back propagation of the scattered field. This is the same back propagation effect for the plane wave spectrum representation of the Green's function in (6), which amplifies exponentially the noise carried by the evanescent modes of the scattered fields [17, 18]. It is almost impossible to obtain the original permittivity distribution, since the small numerical errors existing in this moment method inversion are amplified exponentially in the back propagation process if all the modes of the scattered field are included in the inversion. By filtering out all these higher-order modes and keeping only the lower-order modes of $|m| \leq M$, where are M is the smallest integer making the argument in (10) about one as

$$M \geq ek_0\rho_n/4. \tag{11}$$

For the maximum radius of the scatterer $\rho = D/2$, the inversion is stabilized in the presence of noise and errors in the scattered field and

any other additional regularization processes are not needed.

In order to see the various limitations of the iterative inversion methods, the cost functionals defined in (7) and (8) are calculated as a function of the relative permittivities of the cells ϵ_n and the object size D. The cost functionals for the fields scattered by a homogeneous circular cylinder of relative permittivity $\epsilon = 2$ may be calculated as a function of the relative permittivity distribution ϵ_n, as shown in Figure 2, by assuming that the measured fields are equal to the exact analytic solution for a plane wave incidence. Three cost functionals in Figure 2 are for three different sizes of the object diameter D equal to 1λ, 2λ, and 4λ, where λ is the free space wavelength of the source. It shows that only one global minimum occurs at $\epsilon_n = 2$ and many local minima for other values of ϵ_n depending on D. When the initial values of all ϵ_n are set to 1, the global minimum may be found at $\epsilon = 2$ from Figure 2 by the **LM** algorithm for the diameter of the dielectric cylinder $D = 1\lambda$. For the other diameters larger than 1λ the **LM** algorithm finds the values of the nearest minimum from $\epsilon_n = 1$, that is, $\epsilon_n \approx 0.7$ for 2λ and 1.3 for 4λ.

In order to find the profile distribution of the given object scatterer, one needs the algorithm to find the global minimum of the cost functional. **LM** algorithm, however, may be terminated in one of the local minima since it depends upon the initial profiled distribution. The simulated annealing (**SA**) algorithm [7, 9] and the genetic algorithm (**GA**) [8, 10] are used to find the global minimum successfully. A hybrid algorithm combining either **SA** or **GA** with **LM** algorithm is used to find the global minimum of the cost functional more effectively for the reconstruction of the large and high-contrast penetrable object such as the scattering object of 3λ by 3λ having relative dielectric constant $\epsilon_r = 4.0$ when 10% Gaussian noise is assumed in the measured scattered fields [9, 10]. If the **LM** algorithm traps in one of the local minima, this hybrid algorithm switches **LM** to either **SA** or **GA** to find another permittivity distribution corresponding to the lower cost functional and switches to **LM** again to minimize the functional to reach the deeper minimum and repeats the process until the global minimum is found.

Figure 3 shows how the cost functional changes with the number of angular spectral modes. The cost functional is calculated for a circular dielectric cylinder of diameter 2λ and a relative permittivity of 9. The cost functional with 17 modes, which is the total number of effective

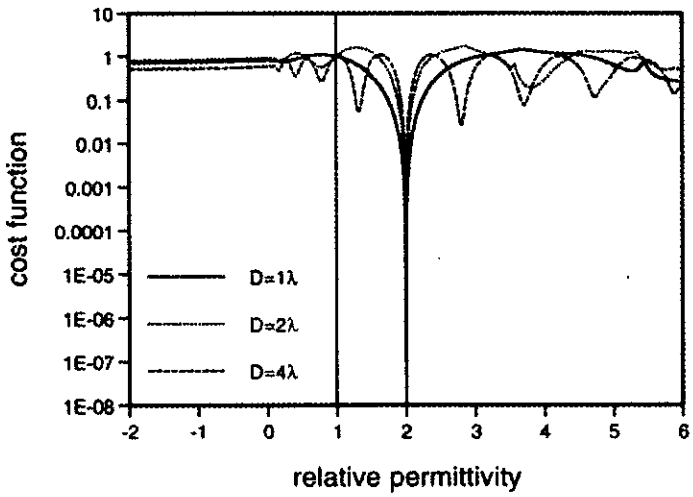

FIGURE 2. Cost functional for a circular dielectric cylinder of (a) $\epsilon = 2$ and its diameter D as parameter.

modes, shows the distinctive global minimum at $\epsilon = 9$ and overlaps with that of 31 modes, even in the presence of 5% Gaussian noise in the scattered fields. Very deep local minima indistinguishable from the global minimum exist with a 1 mode cost functional. In the presence of noise, the local minima of the cost functional are deepened, and the global minimum is shallowed and shifted to the slightly different values of relative permittivity. One may speculate that more data points larger than the effective modes do not improve the reconstruction by the iterative minimization even in the presence of noise in the scattered fields. In the presence of noise it is easier to trap in the local minimum, and the reconstructed distribution of permittivities may be deviated slightly.

From the cost functional obtained by an arbitrary dielectric cylinder it is shown that a single global minimum of the cost functional occurs when the total number of the cells of the scatterer N is smaller than KP, where K is the number of multiple views of different frequencies, $K = I + J$, and P is the total numver of modes used, $P = 2M + 1$. It is shown numerically that multiple global minima occur in its cost functional if $N > KP$, which prohibits the convergence of the reconstruction to the original profile.

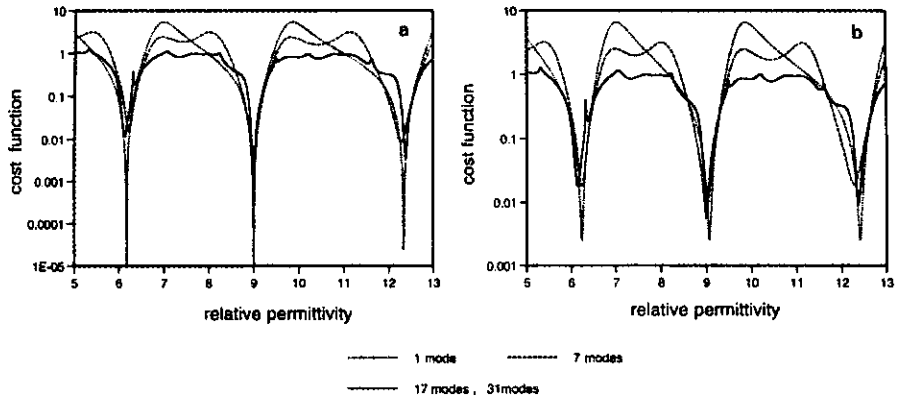

FIGURE 3. Cost functional versus relative permittivity as a function of the number of angular spectral modes for a circular dielectric cylinder of $\epsilon = 9$ and $D = 2\lambda$. (a) Without noise and (b) with 5% Gaussian noise in the scattered fields.

4. Sampling theorem, super resolution, and uniqueness

Iterative inversion of the two-dimensional thin dielectric object distributed along the y-axis excited by a line source, as shown in Figure 4, may be used to show the relationship between the resolution of the reconstruction and the sampling of the measured data. The scattered fields in the plane of $x = d$ in Figure 4 are numerically calculated by the method of moments and used for the measured scattered fields for the iterative inversion. By taking the Fourier transform of the measured scattered fields $u_M^S(d, y)$ in y, one obtains its spatial frequency spectrum $u_M^S(d, \beta)$ as

$$u_M^S(d,\beta) = \int_{-\infty}^{\infty} dy e^{-j\beta y} u_M^S(d,y), \tag{12}$$

where β is the spatial frequency in y-direction. The measured spatial spectrum $U_M^S(d, \beta)$ in the plane of $x = d$ may be transformed into that in the plane of $x = 0$, where the scatteing object is located, via equation in (5) as

$$U_M^S(0,\beta) = U_M^S(d,\beta) e^{j\sqrt{k_0^2-\beta^2}d}, \; I_m\sqrt{k_0^2-\beta^2} < 0, \tag{13}$$

where I_m stands for the imaginary part of.

The scattered fields may be measured at equally-spaced points in y by the interval of Δy such that

$$N(\Delta y) = L, \tag{14}$$

where N and L are the total number and the total length of the measurements in y in the plane of $x = d$. The Fourier transform of the N equally-spaced data of the scattered fields is periodic with period 2π and may be sampled by the same N equally-spaced spatial frequencies for one period by the interval of $\Delta\beta = \frac{2\pi}{L}$ such that its discrete Fourier series reproduces the original discretized scattered fields repeatedly by the period of L. Then one obtains

$$(\Delta y) = \frac{L}{N} = \frac{L}{\left(\frac{B}{\Delta\beta}\right)} = \frac{2\pi}{B},\ \Delta\beta = \frac{2\pi}{L}, \tag{15}$$

where B is the total bandwidth of the spatial frequencies.

Filtering the evanescent modes of the measured scattered fields out and keeping its propagating modes gives $-k_0 \leq \beta \leq k_0$ and $B = 2k_0$. The relationship in (13) between the measured spectrum in the plane of $x = d$ and back propagated spectrum in the object plane of $x = 0$ is essentially the same with different phase term from that of x=d which gives the resolution(Δy) in the object plane from (15) as

$$(\Delta y) = \frac{2\pi}{B} = \frac{2\pi}{2k_0} = \frac{\lambda}{2}, \tag{16}$$

where λ is the wavelength in free space.

For the super resolution such as $\Delta y \sim 0.1\lambda$, the required bandwidth in (19) becomes $B = 2\pi/0.1\lambda = 10k_0$ which requires the measurements of the evanescent modes in addition to all the propagating modes since $\beta > k_0$. Numerical examples of 24 cell reconstruction shown in Figure 5a shows that the error of reconstruction increases as the distance of the measurement plane(d) increases since its bandwidth $B = 5k_0$ includes the evanescent modes, where its resolution $(\Delta y) = 0.2\lambda$ is used for the reconstruction. Figure 5b shows that the root mean square error of the reconstruction increases as the resolution of reconstruction increases when the measurement plane is 2λ apart. This shows clearly that the large error occurs for the resolution of reconstruction smaller than 0.5λ which needs the measurement of evanescent modes.

The cost functionals for the fields scattered by a homogeneous circular cylinder shown in Figure 3 shows that one global minimum exists if

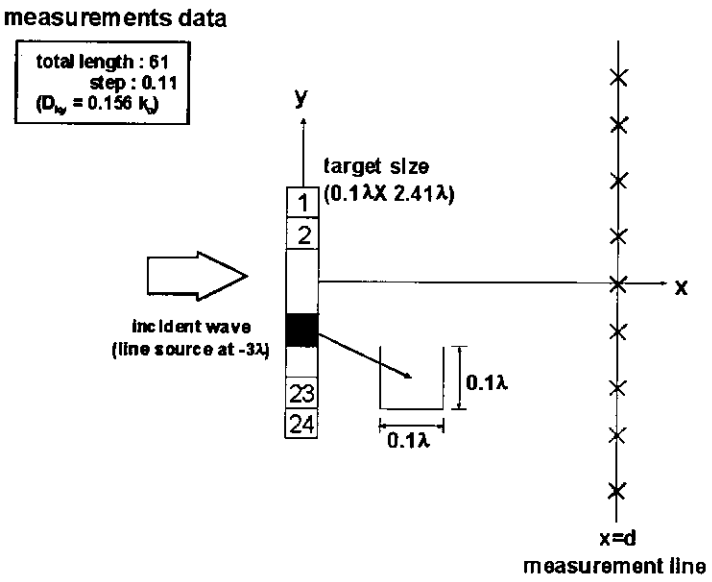

FIGURE 4. Iterative inversion from the planar measurement of the scattered fields.

the number of modes of the measured scattered field exceeds the total number of unknowns. 5% Gaussian noise added to the scattered fields does not change the location of the global minimum of the cost functional much if the higher order modes are filtered out. This implies that the cost functional at the global minimum is bounded if the sufficient number of propagating modes are used as

$$\sum_{i=1}^{I}\sum_{j=1}^{J}\sum_{m=-M}^{M}|F_{ijm}|^2 < \delta, \tag{17}$$

where δ is a constant by the measurement error. Keeping all the propagating modes means the finite resolution of 0.5λ and the distribution of permittivities of the scattering object discretized by the cells of resolution 0.5λ may be obtained by making $F_{mij} = 0$ in (7) and (8) as

$$\frac{a_m(\rho;\omega_i,\phi_j)}{H_m^{(2)}(k_0\rho)} = \frac{j\pi k_0 a}{2}J_1(k_0 a) \sum_{n=1}^{N}(\epsilon_n - 1)u_n(\omega_i,\phi_j)J_m(k_0\rho_n)e^{-jm\phi_n}, \tag{18}$$

where the total number of equations in (18) becomes $2M + 1 + I + J$, since $2M + 1, I$, and J are the total number of m, i, and j, respectively. This gives a unique reconstruction of N unknowns for $(\epsilon_n - 1)u_n$, if the total number of equations, $2M + 1 + I + J = N$, since we have N linear independent algebraic equations for N unknowns.

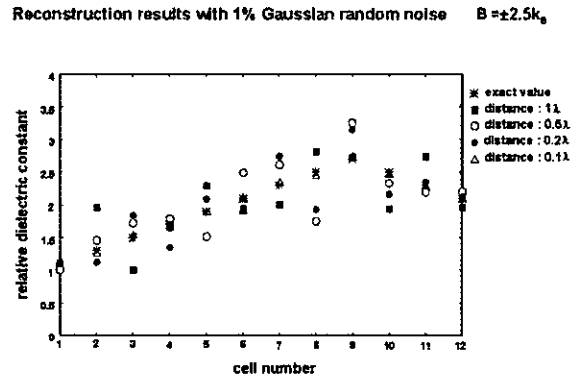

(a)

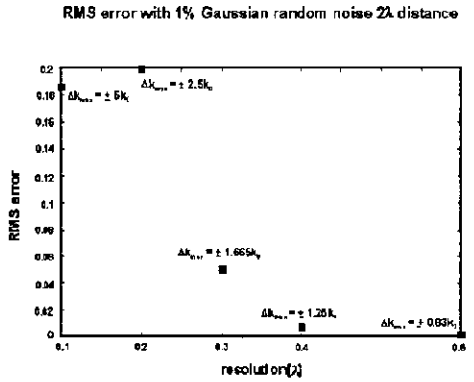

(b)

FIGURE 5. Iterative reconstruction of dielectric profile of 24 cells in Figure 4. (a) Bandwidth is fixed by $5k_0$ and the distance of the measurement plane changes from 0.1λ to 1λ when 1% of Gaussian noise is present in the scattered fields. (b) RMS reconstruction error increases as the resolution increases from 0.6λ to 0.1λ when the measurement distance is fixed by 2λ and 1% Gaussian noise is present in the scattered fields.

References

[1] M. Slaney, A. C. Kak, and L. E. Larsen, *Limitation of Imaging with First-Order Diffraction Tomography*, IEEE Trans. Antennas Propag. **14** (1966), 460–464.

[2] D. K. Ghodgonkar, O. P. Gandhi, and M. J. Hagmann, *Estimation of Complex Permittivities of Three-Dimensional Inhomogeneous Biological Bodies*, IEEE Trans. Microwave Theory Tech. **31** (1983), 442–446.

[3] A. N. Tikhonov and V. Y. Arsenin, *Solutions of Ill-Posed Problems*, Winston, Washington, D. C., 1977.

[4] J. M. Lee, S. Y. Kim, and J. W. Ra, *A Spectral Inverse Technique for Reconstruction of Complex Permittivity Profiles*, Electron. Lett. **24** (1988), 556–558.

[5] S. Caorsi, G. L. Gragnani, and M. Pastorino, *Two-Dimensional Microwave Imaging by a Numerical Inverse Scattering Solution*, IEEE Trans. Microwave Teory Tech. **38** (Aug. 1990), 981–989.

[6] J. E. Jr. Dennis, *Numerical Methods for Unconstrained Optimization and Nonlinear Equations*, Prentice-Hall, Englewood Cliffs, N. J., 1983.

[7] L. Garnero, A. Franchogis, J. P. Hugonju, C. Pichot, and N. Joachimowicz, *Microwave Imaging-Complex Permittivity Reconstruction by Simulated Annealing*, IEEE Trans. Microwave Theory Tech. **39** (Nov. 1991), 1801–1809.

[8] D. E. Goldberg, *Genetic Algorithms in Search, Optimization and Machine Learning, Addison-Wesley*, Reading, MA, 1989.

[9] C. S. Park, S. K. Park, and J. W. Ra, *Moment Method Inversion of Two-Dimensional Complex Permittivity Profiles by Using Effective Modes with Multiple Sources in The Presence of Noise*, Radio Sci. **31** (Nov. - Dec. 1996), 1877–1886.

[10] S. Y. Yang, H. K. Choi, and J. W. Ra, *Reconstruction of a Large and High-Contrast Penetrable Object by Using the Genetic and Lenvenberg-Marquardt Algorthms*, Microwave Opt. Technol. Lett. **16** (Sep. 1997), 17–21.

[11] W. C. Chew, *Waves and Fields in Inhomogeneous Media*, Van Nostrand Reinhold, New York, 1990.

[12] J. H. Richmond, *TE-Wave Scattering by Dielectric Cylinder of Arbitrary Cross-Section Shape*, IEEE Trans, Antennas Propag. **14** (1966), 460–464.

[13] M. Abramowitz and I. A. Stegun (Eds.), *Handbook of Mathematical Functions with Formulas, Graphics, and Mathematical Tables*, Dover, Mineola, N. Y., 1972.

[14] K. S. Lee and J. W. Ra, *Angular Spectral Inversion for Reconstruction of Complex Permittivity Profiles*, Microwave Opt. Technol. Lett. **5** (Aug. 1992).

[15] K. Miller, *Least Squares Methods for Ill-Posed Problems with a Prescribed Bound*, SIAM J. Math. Anal. **1** (1970), 52–74.

[16] N. Joachimowicz, C. Pichot, and J. P. Hugonin, *Inverse Scattering: An Iterative Numerical Method for Electromagnetic Imaging*, IEEE Trans. Antennas Propag. **39** (Dec. 1991), 1742–1752.

Department of Electrical Engineering and Computer Science
Korea Advanced Institute of Science and Technology
373-1, Kusong-Dong, Yusong-Gu, Taejon 305-701, Korea
E-mail: rawoong@ee.kaist.ac.kr